4f Electrons and the formation of the ground state in the Kondo insulator CeNiSn

P. A. Alekseev, E. S. Klement'ev, V. N. Lazukov, E. V. Nefedova, I. P. Sadikov, and M. N. Khlopkin

Kurchatov Institute, 123182 Moscow, Russia

A. Yu. Muzychka and I. L. Sashin

Joint Institute of Nuclear Research, 141980 Dubna, Moscow Region, Russia

N. N. Efremova

Institute of the Physics of Metals, 620219 Ekaterinburg, Russia

W. Bührer

PSI, CH-5232, Villigen, Switzerland
(Submitted 30 June 1994)
Zh. Eksp. Teor. Fiz. **106**, 1228–1245 (October 1994)

The conditions for the formation of the ground state of $4f$ electrons in CeNiSn and the effect of the $4f$ electrons on the magnetic excitation spectrum and on the lattice properties (thermal expansion and lattice dynamics) were investigated by means of inelastic neutron scattering, x-ray diffraction, and L_{III} absorption spectroscopy. It was determined that the Ce ions in CeNiSn are in an unstable-valence state, falling between the classical intermediate-valence and heavy-fermion systems, with the characteristic energy $E^* \approx 4$ meV. The splitting of the ground state multiplet of Ce^{3+} ions in the crystalline field of RNiSn was determined to be 14 meV. The energy of the first excited state was found to be close to the energy of spin fluctuations of the $4f$ electrons. The structure of the wave functions of the $4f$ multiplet of the cerium ions and the closeness of the energies interaction in the crystal electric field and the spin fluctuation energies are consistent with the hypothesis that the crystal field excitations are hybridized with Kondo excitations. It was found that the lattice properties of CeNiSn are qualitatively different from those of LaNiSn, because of both the specific nature of the LaNiSn lattice and the valence instability of the cerium ions. Experimental results confirming that the gap in the electronic spectrum of CeNiSn is formed by a coherent mechanism were obtained for $Ce_{1-x}La_xNiSn$.

1. INTRODUCTION

In recent years a new class of compounds—the so-called Kondo insulators—has aroused great interest.[1] These compounds are based on elements whose f-shell is partially filled. The magnetic and thermodynamic properties exhibit features that are similar to anomalies characteristic of heavy-fermion and intermediate-valence systems. This similarity indicates that the state of the f-electrons in Kondo insulators is unstable. A typical example is the intermetallic system CeNiSn (the first member of the class of cerium-based compounds), in which a gap (pseudogap) with energy $E_g \approx 5$ K forms in the electron density of states at the Fermi level in the limit $T \to 0$.[2,3] The strong interaction of the $4f$-electrons of cerium in CeNiSn with the conduction electrons results in a large electronic contribution to the heat capacity [$\gamma = 200$ mJ/(K^2 mole) (Ref. 2 and 3)], as is typical of heavy-fermion systems. The magnetic susceptibility approaches a finite value as $T \to 0$: $\chi(T \to 0) = 15$ mole^{-1} (Ref. 2). These properties were attributed to the formation of an intermediate valence state of the Ce ions,[2] while elsewhere[4] CeNiSn was considered to be a heavy-fermion system. In summary, on the basis of the available experimental data, this material cannot be classified unequivocally as an intermediate-valence or heavy-fermion system.

In spite of a large amount of experimental work on CeNiSn (see Ref. 2 and references cited there) in which mainly the effect of the gap on different properties was studied, the role of the interactions of the f-electrons with the conduction electrons and with the crystal field, which are critical to the formation of the ground state of the system, has remained virtually unstudied.

In the present work we investigated, by means of inelastic neutron scattering, x-ray diffraction, L_{III} absorption spectroscopy, and measurements of the heat capacity, the state of the $4f$-electrons and the effect of their basic interactions on the spectrum of magnetic excitations and on the lattice properties (thermal expansion and lattice dynamics) of CeNiSn. We also analyzed the relationship between the valence state of the Ce and the suppression of the gap in the electron spectrum when La is substituted for Ce. The interaction energy of the $4f$-electrons with the conduction electrons and with the crystal field were determined experimentally, and information was obtained about the wave functions of the low-energy states of the Ce ion in CeNiSn.

2. SAMPLES AND MEASUREMENT PROCEDURE

The compound CeNiSn has an orthorhombic crystal lattice of the type ε-TiNiSi with space group[5] *Pnma* or, ac-

 1063-7761/94/100665-10$10.00

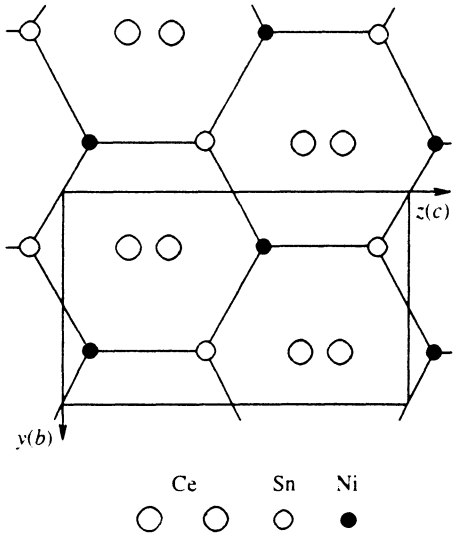

FIG. 1. Crystal lattice of the CeNiSn system in projection on the yz (bc) plane. The hatched circles represent Ce ions located near the $x=0$ plane; the open circles represent Ce ions located near the $x=0.5$ plane. The Ni and Sn ions illustrated in the figure are located close to the $x=0.75$ plane. One other "fluted" plane of Ni and Sn atoms with $x=0.25$ differs from the $x=0.75$ plane in that the Ni and Sn ions are interchanged.

cording to the results of the latest structural work, a lattice with a distorted symmetry of this type with the space group $Pn2a$.[6] The local environment of the rare-earth (RE) ions in CeNiSn has monoclinic symmetry with the point group C_s. Figure 1 displays the structure of CeNiSn in projection on the $yz(bc)$ plane.

In the present work we investigated isostructural polycrystalline samples of RNiSn (R=Ce, La, Y, Pr, Nd). The single-phase nature of the samples and their correspondence to the CeNiSn structure were established by x-ray and neutron diffraction.

The neutron diffraction patterns were obtained on the DISK x-ray diffractometer (Kurchatov Institute IR-8 reactor) at $T=300$ K for CeNiSn and LaNiSn samples. The parameters of the positions of the rare-earth ions and the Ni and Sn ions, determined by the Rietvelt full-profile analysis method, were found to be close to the values presented in Ref. 5.

The inelastic thermal-neutron scattering experiments, whose purpose was to study the magnetic and lattice excitations, were performed on a KDSOG time-of-flight spectrometer with a fixed neutron energy ($E_f=4.9$ meV) (IBR-2, Joint Institute of Nuclear Research, Dubna) on $Ce_{1-x}La_xNiSn$ ($x=0$, 0.1, 0.3, 0.7, 1) and $Nd_{0.3}La_{0.7}NiSn$ samples at temperatures of 10, 80, and 300 K. The scattering angles 2θ ranged from 30° to 90° and the energy resolution near the elastic peak was 0.5 meV.

The temperature dependence of the crystal field effects for $Nd_{0.3}La_{0.7}NiSn$ were investigated in detail on a TAS-5 three-axis spectrometer (SAPHIR reactor, ETH and PSI, Switzerland) at a fixed analyzer energy $E_a=14.95$ meV by the $Q=$const method at temperatures $T=10$, 30, 60, and 100 K and momentum transfer $Q=1.5$, 4.3, and 4.65 Å^{-1}.

The masses of the samples for the neutron measurements ranged from 40 to 150 g (KDSOG) and 10 g (TAS-5).

The temperature dependence of the lattice parameters was studied by the method of x-ray diffraction. The x-ray diffraction patterns of polycrystalline samples of $Ce_{1-x}La_xNiSn$ ($x=0$, 0.05, 0.3, 0.5, and 1), $La_{0.7}Y_{0.3}NiSn$, and PrNiSn were obtained on a SIEMENS D500 diffractometer[7] and a DRON-3 diffractometer (CuK_α FeK_α lines) at temperatures ranging from 10 to 300 K. The (020), (013), (303), (222), and (033) Bragg reflections in the range of angles 2θ from 38° to 80° were used to determine the lattice parameters a, b, and c. An internal standard (silicon) was used to eliminate the systematic error in the angular positions of the reflections. The lattice parameters were calculated by solving a system of normal equations, which included a collection of the angular positions of all measured Bragg reflections with weighting factors that account for the measurement accuracy. The temperature dependences of the linear thermal expansion coefficients (LTECs) $\alpha_{a_i}=(1/T)da_i/dT$ $(a_i=a,b,c,)$ were determined by differentiating presmoothed temperature dependences of the lattice parameters. The lattice parameters were determined with the relative accuracy $\delta a_i/a_i=1.5\cdot10^{-4}$ (SIEMENS diffractometer) and $4\cdot10^{-8}$ (DRON-3 diffractometer). The error in the linear thermal expansion coefficients was 4 and $12\cdot10^{-6}$ K^{-1}, respectively.

The temperature dependence of the heat capacity for the $La_{0.7}Y_{0.3}NiSn$ and LaNiSn samples at temperatures ranging from 3 to 110 K was measured by the adiabatic method.[8] The relative error of the measurements did not exceed 3%.

The valence of Ce was measured by means of L_{III} x-ray absorption spectroscopy. The spectra were obtained at $T=300$ K in the second order of reflection from the $(10\bar{1}1)$ plane of a quartz crystal. The energy resolution was ≈8000. The spectra were recorded by a scheme similar to the one described in Ref. 9.

3. EXPERIMENTAL RESULTS AND DISCUSSION

3.1. Spectrum of magnetic excitations in $Ce_{1-x}La_xNiSn$

The magnetic components of the spectral scattering function $S_{mag}(E)$, averaged over the scattering angles from 30° to 90°, as a function of the energy transferred by the neutron for CeNiSn ($T=10$ and 80 K) and $Ce_{0.7}La_{0.3}NiSn$ ($T=10$ K) samples, are displayed in Fig. 2. The magnetic component was identified by subtracting out the phonon contributions to the spectral scattering function. The phonon component was estimated from measurements at $T=300$ K and from the LaNiSn neutron scattering spectra, in which there is no magnetic scattering component. It is obvious from Fig. 2 that the spectrum of the magnetic response of the CeNiSn system at $T=10$ K does not have any distinct peaks associated with transitions between the levels of the $4f$-multiplet of the Ce ions in the crystal field. The intensity of magnetic scattering by CeNiSn changes slightly when La is substituted for Ce (see the spectrum of the $Ce_{0.7}La_{0.3}NiSn$ sample). The energy dependence $S_{mag}(E)$ for all samples ($x=0$, 0.1, 0.3, and 0.7) at temperatures of 10 and 80 K is described well by a Lorentzian spectral function (for $x=0$ and 0.3 this result was obtained previously in Ref. 10) centered at $E=0$ meV (E is the energy transferred by the scat-

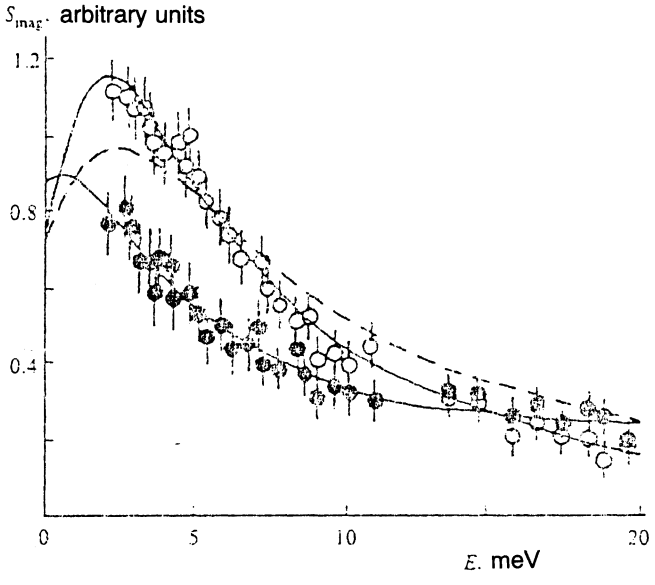

FIG. 2. Magnetic components of the spectral neutron-scattering functions for CeNiSn at $T=10$ K (○) and $T=80$ K (●). The curves represent the best fit of the experimental points by a quasielastic Lorentzian spectral function. The dashed curve represents the best fit for $Ce_{0.7}La_{0.3}NiSn$ ($T=10$ K).

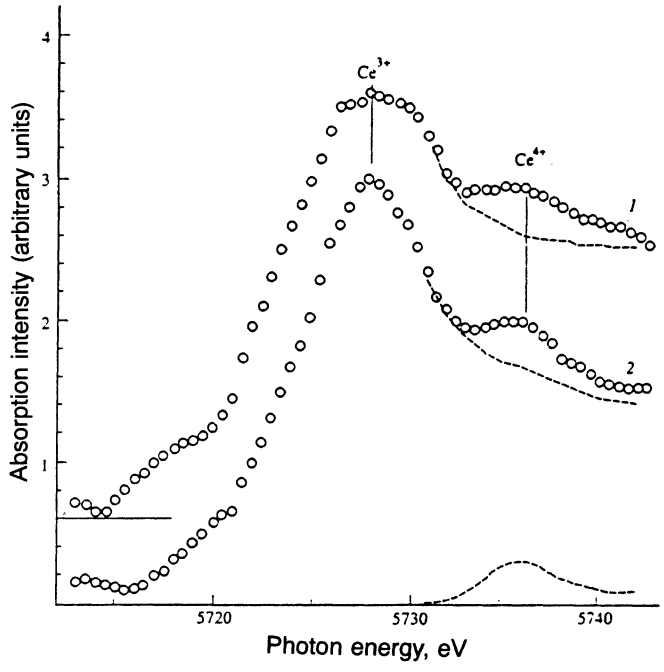

FIG. 3. L_{III}-edge absorption spectra of Ce in CeNiSn (*1*) and in $Ce_{0.5}La_{0.5}NiSn$ (*2*). The dashed curve represents the contribution of the Ce^{4+} state for CeNiSn.

tered neutron) and with a temperature factor which appears as a result of the principle of detailed balance:

$$S_{mag}(E) \propto E\left[1-\exp\left(-\frac{E}{kT}\right)\right]^{-1}\frac{\Gamma}{2}\left[E^2+\left(\frac{\Gamma}{2}\right)^2\right]^{-1}, \quad (1)$$

where $\Gamma/2$ is the half-width at half-height. The variation in the spectra with increasing temperature is due mainly to variations in the temperature-dependent factor, while in the range 10–80 K the half-width of the peak ($\Gamma/2=3.5\pm1$ meV for CeNiSn and 4.1 ± 1 meV for $Ce_{0.7}La_{0.3}NiSn$) is temperature independent within the limits of experimental accuracy. The gap in the spectrum of magnetic excitations of CeNiSn and the gap-associated excitation at an energy of about 2 meV, which were found near the (001) direction in the neutron experiments on single crystals,[11,12] are not manifested in the spectra obtained, since polycrystalline samples were investigated over a different temperature range.

Thus the magnetic scattering observed for the $Ce_{1-x}La_xNiSn$ samples is described well by a quasielastic Lorentzian spectral function with a half-width of about 4 meV. A magnetic response of this type is characteristic of neutron scattering spectra under conditions of rapid spin fluctuations.[13] The half-width of the quasielastic spectral response makes it possible to estimate the characteristic energy of the spin fluctuations as $E^*\approx4$ meV. The value obtained for $\Gamma/2$ lies between the values of $\Gamma/2$ for typical intermediate-valence systems[13] (10 and more meV) and heavy-fermion systems[13] (0.1–1.0 meV at $T=10$ K). As far as the temperature dependence of the half-width is concerned, up to 80 K, $\Gamma/2$ for CeNiSn does not change, within the limits of the measurement error, with increasing temperature. Such a weak temperature effect on the quasielastic scattering is, to a high degree, characteristic of intermediate-valence systems. The value obtained for $\Gamma/2$ from the neutron spectra can be compared to the measurements of the magnetic susceptibility on the basis of the assumption that the magnetic scattering is described by a single Lorentzian spectral function.[14] From the Kramers–Kronig relation for the static and dynamic magnetic susceptibilities

$$\chi_{st}(T)=\frac{1}{\pi}\int_{-\infty}^{\infty}\frac{\chi''(E,T)}{E}\,dE, \quad (2)$$

as well as the relation between $\chi''(E)$, the cross section for magnetic scattering, and the spectral scattering function for neutrons[15]

$$\sigma_{mag}(T)\propto\int_{-\infty}^{\infty}[1-\exp(-E/kT)]^{-1}\chi''(E,T)dE, \quad (3)$$

$$S(E,T)\propto\chi''(E,T)[1-\exp(-E/kT)]^{-1}, \quad (4)$$

we obtain, setting $\chi_{st}=1.54\cdot10^{-2}$ mole^{-1} ($T=10$ K),[3] the value $\Gamma/2=3.98$ meV, which is in good agreement with the value determined experimentally from inelastic neutron scattering at $T=10$ K (a Lorentzian spectral function was integrated up to energy 0.5 eV). The good agreement between the experimental value of $\Gamma/2$ and the value computed from the susceptibility shows that the assumption made is acceptable.

Two peaks, corresponding to the states Ce^{3+} and Ce^{4+}, are observed in the L_{III}-edge absorption spectra (Fig. 3). Such spectra are indicative of an intermediate-valence state of cerium in CeNiSn. The intensities of the peaks make it possible to estimate the valence for CeNiSn: $\nu=3.12\pm0.04$ ($T=300$ K). The ratio of the intensities is essentially the

same for $Ce_{0.5}La_{0.5}NiSn$. Therefore, the valence of cerium does not change when La is substituted for Ce.

The compound CeNiSn can thus be characterized as a system in which the state of the $4f$-electron shell is near the boundary of the intermediate-valence and heavy-fermion regimes. The neutron measurements indicate that in CeNiSn the valence of Ce is different from 3+ at low temperatures, and they agree qualitatively with the $T=300$ K L_{III}-spectroscopy data ($\nu=3.12\pm0.04$), i.e., the value obtained for the valence corresponds more to the intermediate-valence regime.

When La is substituted for Ce in $Ce_{1-x}La_xNiSn$, the gap in the electronic spectrum vanishes,[16] but for $x>0.1$ no qualitative changes were observed in the magnetic-excitation spectra (at $T=10$ and 80 K) or the L_{III} spectra (300 K). From this it can be concluded that the suppression of the gap is not associated with the change in the valence state of cerium, but the existence of the gap is not merely a direct consequence of just the intermediate valence. This is an important argument in favor of a coherent mechanism for the formation of the gap in the electron spectrum. Indeed, the substitution of a small number of La ions for Ce ions in the lattice has virtually no effect on the single-ion properties of Ce, but it destroys the regularity of the rare-earth sublattice.

3.2. Crystal potential in RNiSn

To estimate directly the interaction energy of the $4f$-electron shell of Ce ions with the crystal field in CeNiSn, the Ce ions must be transferred into a state with a localized magnetic moment. In a number of cases the transition into an integer-valence state can be made by expanding the lattice by substituting for the Ce ion La ions whose ionic radius is larger. Measurements of the magnetic-excitation spectra of $Ce_{1-x}La_xNiSn$ samples right up to $x=0.7$ showed that the energy dependence $S_{mag}(E)$ does not exhibit any crystal-field effects, i.e., the Ce ions remain in an intermediate-valence state right up to $x=0.7$. According to Ref. 17, the nearest-neighbor environment of the Ce ions (specifically, the Ce–Ni distance) determines mainly the valence state of the Ce ions in Ce–Ni alloys. The structure of CeNiSn is peculiar in that when La is introduced into the lattice, the distance to the ions closest to the cerium ions remains virtually unchanged. If it is assumed that the results of Ref. 17 are applicable to Ce(La)NiSn, then this is the reason why the Ce ions are not transferred into the Ce^{3+} state.

When Cu, Pt, or Pd is substituted for Ni, the Ce ions are transferred into a state with a localized magnetic moment. This makes it possible to observe effects which are due to the crystalline field,[2,18] but the fact that the nearest-neighbor environment of the Ce ions is different from that in CeNiSn must inevitably change the crystal potential. This makes it impossible to observe directly the splitting of the $4f$-multiplet of the Ce ions in the RNiSn lattice. It was found that the interaction of the $4f$-electrons of cerium with the crystal field in the RNiSn system can be estimated by using a paramagnetic marker,[19] i.e., by introducing Nd ions into the RNiSn lattice, which have a localized magnetic moment. The neutron spectra were measured for $Nd_{0.3}La_{0.7}NiSn$, which is equivalent to CeNiSn from the standpoint of the nearest neighbor environment of the rare-earth ions and inter-ion distances. The magnetic components of the spectral neutron-scattering functions for this sample for $Q=1.5$ Å^{-1} at $T=10$ and 100 K are displayed in Fig. 4. The phonon spectrum, obtained by analyzing the neutron scattering spectra measured at $T=100$ K for two values of momentum transfer, $Q=1.5$ and 4.65 Å^{-1}, for this sample was used to determine the magnetic component. The experimental spectra were separated into the magnetic and phonon components on the basis of the fact that the different dependences of the magnetic and phonon scattering intensities on the transferred momentum are different. The magnetic form factor for the Nd^{3+} ions decreases rapidly with increasing Q, while the intensity

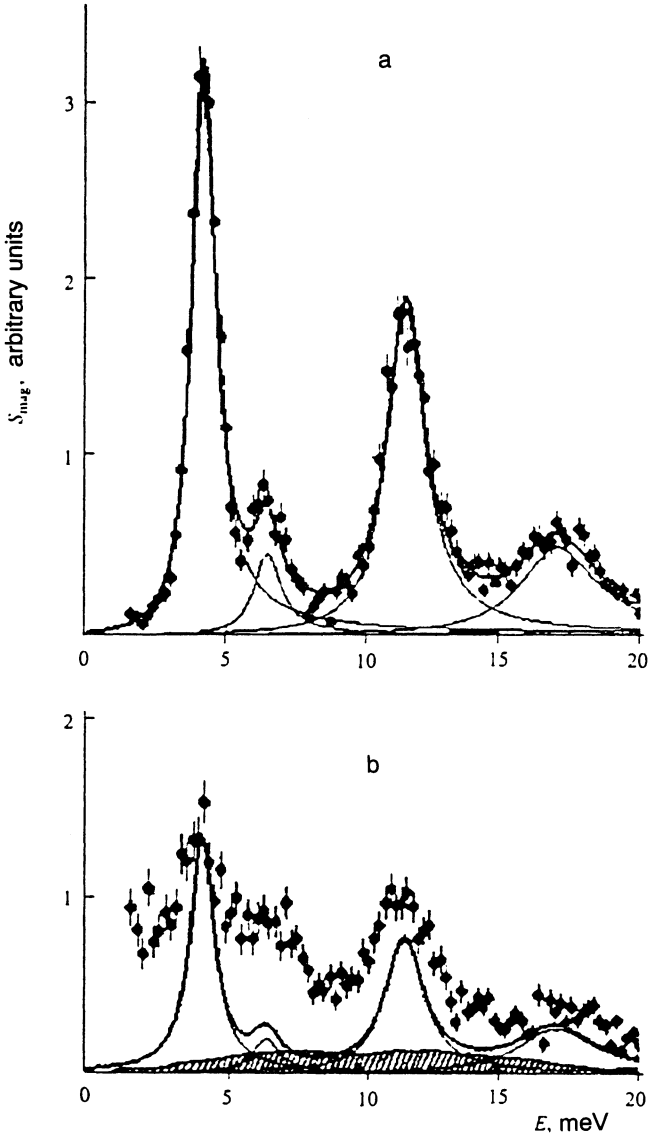

FIG. 4. Magnetic components of the spectral neutron-scattering function for $Nd_{0.3}La_{0.7}NiSn$ at $T=10$ K (a) and 100 K (b). The dots represent the experimental data obtained with the TAS-5 spectrometer. The thick curve in (a) is the envelope of the best fit of the peaks using four Lorentzian curves; the thin curve in (b) is the envelope of the transition intensities under the assumption that all peaks in the $T=100$ K spectrum correspond to transitions solely out of the ground state. The hatched region illustrates the phonon component at $T=100$ K.

TABLE I. Experimental values of the ratio $|M_{ij}|^2/|M_{12}|^2$.

i	j				
	1	2	3	4	5
1	1.36 ± 0.70	1	0.16 ± 0.05	0.91 ± 0.17	0.52 ± 0.14
2	-	-	0.81 ± 0.26	0.78 ± 0.45	0.74 ± 0.60
3	-	-	-	0.07 ± 0.11	1.36 ± 1.10
4	-	-	-	-	4.20 ± 3.60
5	-	-	-	-	-

Note. Here $|M_{ij}|^2=|\langle\Gamma_j|\hat{J}_p|\Gamma_i|^2$, Γ_i, and Γ_j are the initial and final states of the $4f$-multiplet, and $\hat{J}_p$ is the perpendicular component of the angular-momentum operator.

of the phonon scattering component is directly proportional to the squared momentum transfer. The procedure for separating the contributions reduced to solving the following system of linear equations for each experimental point (labeled by the subscripts i):

$$S^{1.5}_{mag}(E_i)+S^{1.5}_{ph}(E_i)=S^{1.5}(E_i),$$

$$\frac{F^2(4.65)}{F^2(1.5)}S^{1.5}_{mag}(E_i)+\left(\frac{4.65}{1.5}\right)^2 S^{1.5}_{ph}(E_i)=S^{4.65}(E_i), \quad (5)$$

where $F(Q)$ is the magnetic form factor for Nd^{3+},[20] and the superscripts indicate the values of Q. The correctness of this procedure depends on the fraction of the coherent component of the inelastic nuclear scattering. To make an additional check of the correctness of the separation on the basis of the phonon and magnetic contributions obtained for $Q=1.5$ and 4.65 Å^{-1}, the neutron scattering spectrum for $Q=4.3$ Å^{-1} and $T=100$ K was calculated. This spectrum was essentially identical to the spectrum measured under these conditions. The $T=100$ K phonon contribution was recalculated at lower temperatures according to a Bose temperature factor. It is obvious from Fig. 4 that the phonon contribution to the neutron scattering spectrum for $T=10$ K and $Q=1.5$ Å^{-1} is small and is less than 5% of the magnetic contribution.

Four peaks are clearly seen in the magnetic component of the spectral neutron-scattering function at the energies $E=4.2$, 6.6, 11.6, and 17.1 meV transferred by neutrons (Fig. 4). These peaks correspond to transitions between levels of the $4f$ multiplet of the Nd^{3+} ions, which the crystal field splits into five Kramers doublets. As the temperature increases, their intensity decreases. This makes it possible to associate all of these peaks with transitions out of the ground state of the split multiplet. As a result, the energies of all transitions and therefore all levels as well as the intensity of the transitions out of the ground state are determined immediately. The intensity of the transitions between the excited states was determined from the temperature dependence of the spectra. By using vanadium as a marker to calibrate the spectra, we were able to determine the matrix elements of the elastic and quasielastic transitions for the ground-state doublet. The experimentally obtained ratios of the squared moduli of the matrix elements, determined from the transition intensities, are presented in Table I.

The nearest-neighbor environment of the rare-earth ions in the case of RNiSn consists of six Ni ions and six Sn ions. As is clearly seen in Fig. 1, the rare-earth ions lie inside slightly distorted hexagonal prisms formed by alternating Ni and Sn ions. The true symmetry of the environment for the positions of the rare-earth ions in orthorhombic RNiSn is monoclinic with the point symmetry group C_s (the only nontrivial symmetry operation is reflection in the yz plane). Because of the smallness of the monoclinic distortions, the nearest-neighbor environment of rare-earth ions can be regarded as having trigonal symmetry with the point group D_{3d} and a threefold rotational symmetry axis parallel to the crystallographic x axis. The next-nearest neighbor coordination sphere formed by the rare-earth ions has a six-fold rotational symmetry axis (neglecting small distortions), i.e., it necessarily has a three-fold axis. Because the symmetry of the environments of the rare-earth ions in RNiSn is close to trigonal, the crystal field can be described with a Hamiltonian for trigonal symmetry. This decreases the number of parameters in the Hamiltonian of the crystal field from 15 (for monoclinic symmetry) to six, if the crystal field is represented in a coordinate system such that the quantization axis is oriented along the three-fold rotational symmetry axis. The crystal-field Hamiltonian for trigonal symmetry[21]

$$\hat{H}=B^0_2\hat{O}^0_2+B^0_4\hat{O}^0_4+B^0_6\hat{O}^0_6+B^6_6\hat{O}^6_6+B^3_4\hat{O}^3_4+B^3_6\hat{O}^3_6, \quad (6)$$

where $\hat{O}^m_n$ are Stevens operators and B^m_n are phenomenological parameters of the crystal field, was diagonalized analytically. The dimension of the problem was reduced to five on the basis of the parameterization proposed in Ref. 22. The deviation of the computed energies of the states of the split $4f$-multiplet of Nd^{3+} and the squared matrix elements of the transitions between the levels from the experimentally determined values was minimized numerically by varying the crystal-field parameters (see Table I). This procedure yielded six parameters that best describe the experimental data, i.e., the energy of the four excited states and the 11 values of the matrix elements. The number of experimentally determined parameters in the measurements is larger than the number of computed parameters B^m_n, so that the neutron spectra can be described uniquely. Figure 5 displays the experimental neutron scattering function for $T=10$ K and the function calculated using six parameters. The good agreement between the experimental results and the calculations confirms the appropriateness of the approach based on the closeness of the local symmetry to trigonal symmetry. The small discrepancies be-

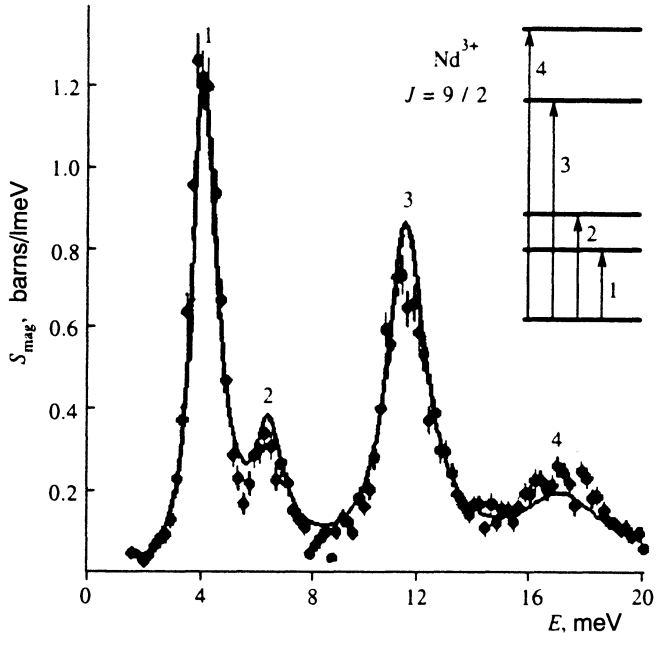

FIG. 5. Experimental (dots) and computed (lines) spectral functions of magnetic neutron scattering in a trigonal crystal field for $Nd_{0.3}La_{0.7}NiSn$ at $T=10$ K. Inset: splitting of the ground $4f$-multiplet of Nd^{3+} ions in a crystal field in $Nd_{0.3}La_{0.7}NiSn$.

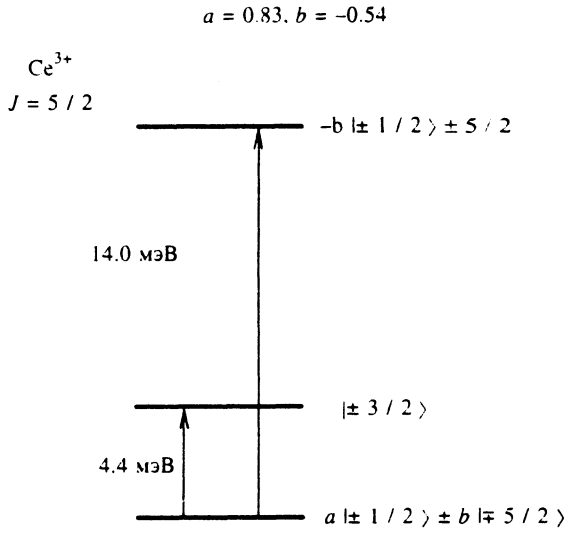

FIG. 6. Computed splitting of the ground $4f$-multiplet of Ce^{3+} ions in the crystal field of RNiSn.

tween the computed spectrum for the transitions 2 and 4 (Fig. 5) and the experimental spectrum in the energy range 5–7 meV and 14–18 meV were probably connected with the fact that monoclinic distortions were neglected. It is interesting to note that the same final parameter set, which describes the crystal potential, was also obtained by lowering the symmetry of the environment from hexagonal to trigonal. In this case, first the Ni and Sn ions were assumed to be equivalent from the standpoint of their contribution to the potential and the problem was solved for a four-parameter Hamiltonian of a hexagonal crystal field. Next, terms with B_4^3 and B_6^3, which account for the difference between the Ni and Sn ions, were added to the parameters being varied, and the complete set of parameters B_n^m was found. The agreement between the results obtained by the two different approaches confirms that the values obtained for the crystal-field parameters are correct.

The parameters in the Hamiltonian of the crystal field which were obtained with the Nd ions were used to calculate the splitting of the $4f$-multiplet of the Ce^{3+} ions in the crystal field in RNiSn taking into account the differences of the electron shells of Ce and Nd ions according to Ref. 21, but neglecting the hybridization with the conduction electrons for cerium. The computed splitting scheme is displayed in Fig. 6. Because of the smallness of the monoclinic distortions, the deviations of the environment of the rare-earth ions from monoclinic symmetry should result in only a small shift of the energy levels and in some mixing of states with angular momentum $J_z=1/2$, 3/2, and 5/2. However, the components of the wave functions obtained in the trigonal approximation still predominate. The ground state is a quantum-mechanical mixture of the states $|\pm 1/2\rangle$ and $|\mp 5/2\rangle$ with a small admixture of $|\pm 3/2\rangle$, and the first excited doublet with the $|\pm 3/2\rangle$ states predominating is split from the ground state by about 4.4 meV. Therefore, the energy splitting between the ground and first excited levels of the multiplet is of the order of E^*, i.e., the energy of spin fluctuations is close to the splitting in the crystal field.

3.3. Lattice properties

To study the possible manifestations of unstable valence in the lattice dynamics of CeNiSn, we measured the inelastic neutron scattering spectra for Ce(La)NiSn. Figure 7 illus-

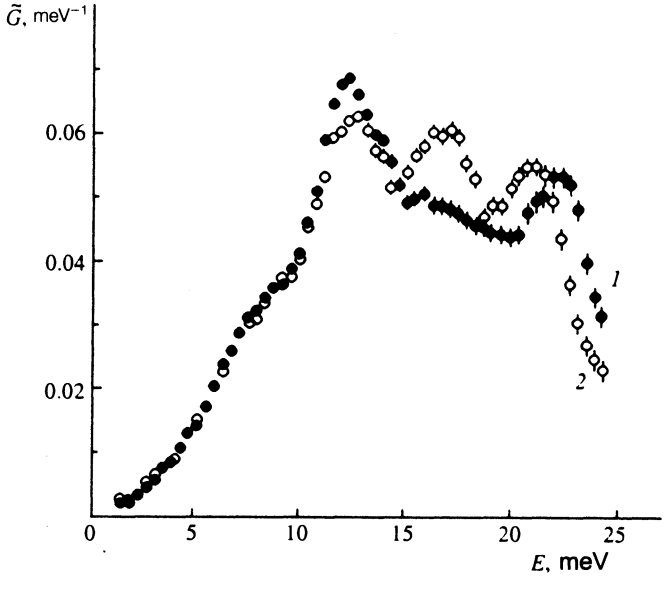

FIG. 7. Generalized phonon density of states $\tilde{G}(E)$ for CeNiSn (*1*) and LaNiSn (*2*).

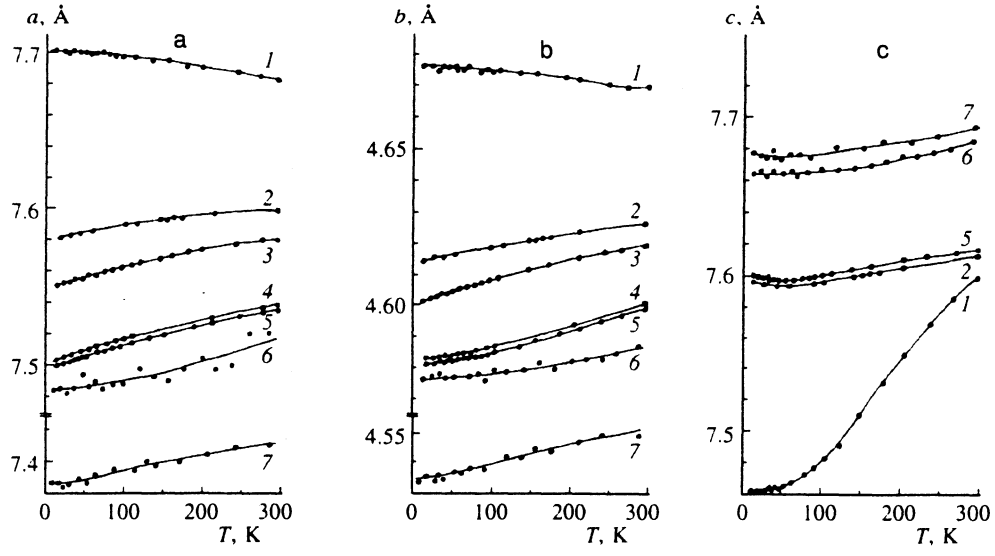

FIG. 8. Temperature dependence of the lattice parameters a (a), b (b), and c (c) for $Ce_{1-x}La_xNiSn$ with $x=1$ (*1*), $x=0.5$ (*2*), $x=0.3$ (*3*), $x=0.5$ (*4*), $x=0$ (*5*), $La_{0.7}Y_{0.3}NiSn$ (*6*), and PrNiSn (*7*).

trates the generalized room-temperature phonon density of states $\tilde{G}(E)$ obtained for CeNiSn and LaNiSn from the $T=300$ K scattering spectra:

$$\tilde{G}(E)=\sum_{i=1}^{s}(\sigma_i/M_i)g_i(E)\Big/\sum_{i=1}^{s}(\sigma_i/M_i), \qquad (7)$$

where $g_i(E)$ is the partial phonon density of states and σ_i and M_i are, respectively, the neutron scattering cross section and the mass of the nuclei in the sample. It is obvious from Fig. 7 that the functions $\tilde{G}(E)$ are, on the whole, similar to one another and are limited in energy to about 25 meV. This limiting energy is relatively low compared to the typical values for nickel-bearing compounds (35–45 meV). Although the CeNiSn phonon spectra are similar to LaNiSn, the energies of the peaks in $\tilde{G}(E)$ are nonetheless different (compare the peaks at 12 and 22 meV). In CeNiSn the high-energy peak is shifted by 1.2 meV toward high energies, while the low-energy peak is shifted by 0.2 meV in the opposite direction. The peak at 17 meV is appreciably suppressed. Since the cell volume in CeNiSn is smaller than in LaNiSn (264 Å^3 versus 272 Å^3), it can be expected that the phonon spectrum is "hardened" (shifted toward high vibrational energies). The high-energy peak in $\tilde{G}(E)$ and the limit of the phonon spectrum are indeed shifted toward high energies in CeNiSn as compared to LaNiSn. In CeNiSn, however, the energy of the low-energy peak is lower. There are two possible reasons for the differences in the lattice dynamics of CeNiSn and LaNiSn.

First, the cerium system contains partially delocalized $4f$- electrons which screen the charges of the neighboring ions and therefore change the interionic interaction potential. It should be noted that thus far, with the exception of the single investigation of $CePd_3$,[23] no experimental consequences of the effect of intermediate-valence state on the lattice dynamics of cerium systems have been found. One possible explanation for this is that the energy E_c of the charge fluctuations is appreciably higher than the energy of the phonon modes ($E_c \approx kE^* \gg \hbar\omega_{ph}$, where the coefficient $k>1$ depends on the magnitude of the valence[24]). In all previously known cerium intermediate-valence systems $E^* \approx 10$–30 meV, while in CeNiSn $E^* \approx 4$ meV. This suggests that the conditions required for the presence of intermediate-valence effects in the lattice dynamics are satisfied.

Second, the fact that the crystal lattice of CeNiSn is different from that of LaNiSn could have an effect. The lattice parameter c is greater than a for the entire isostructural series RNiSn, with the exception of LaNiSn, in which $a>c$.[5] Under the conditions of a strongly anisotropic lattice with a "soft" phonon spectrum, such a difference produces singularities in the lattice properties of LaNiSn as compared to RNiSn (R≠La). These singularities are most pronounced in the experimentally obtained temperature dependence of the lattice parameters displayed in Fig. 8. It is obvious from Fig. 8 that the thermal expansion of CeNiSn is strongly anisotropic. The qualitative difference of the thermal expansion for CeNiSn (previously discovered in Ref. 10) from that of LaNiSn is interesting. The lattice parameters a and b of LaNiSn decrease with increasing temperature, whereas for CeNiSn a and b increase with increasing temperature. This qualitative difference in the temperature dependence of the thermal expansion is extremely unusual, since Ce and La are neighbors in the lanthanide series and have similar ionic radii. Substitution of nonmagnetic yttrium for 30% of the lanthanum, which ordinarily should change only the values of the lattice parameters, in the present case changes the qualitative character of the temperature dependence of the lattice parameters and makes this dependence similar to that for CeNiSn and PrNiSn (Fig. 8). Therefore, as a structural nonmagnetic analog, $La_{0.7}Y_{0.3}NiSn$ is probably closer to CeNiSn than LaNiSn.

The liability of the LaNiSn lattice also follows from the fact that the temperature dependence of the heat capacity changes when yttrium is introduced into LaNiSn. The temperature dependence of the heat capacity $C(T)$ for $La_{0.7}Y_{0.3}NiSn$ and LaNiSn is displayed in Fig. 9. The results

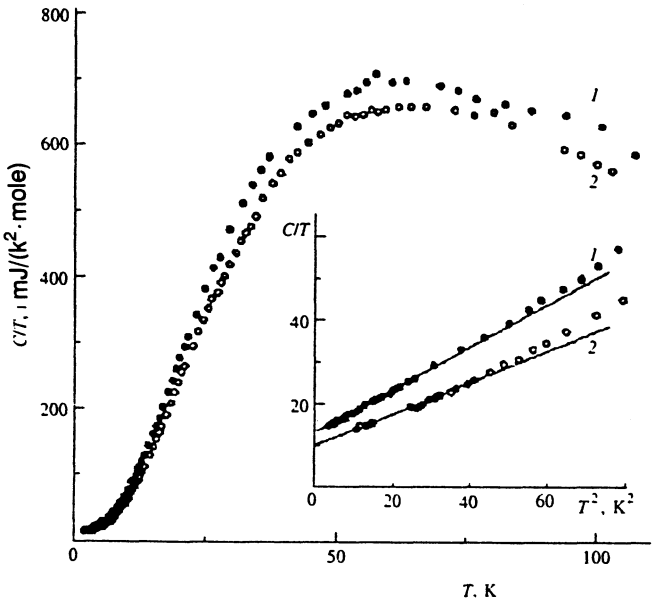

FIG. 9. Temperature dependence of the heat capacity for LaNiSn (*1*) and $La_{0.7}Y_{0.3}NiSn$ (*2*).

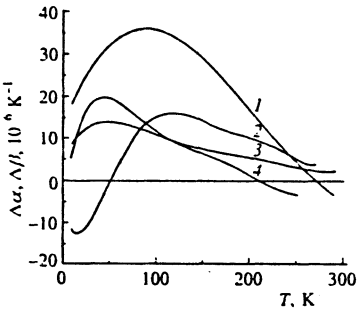

FIG. 10. Difference of the linear and volume thermal expansion coefficients of CeNiSn and its nonmagnetic structural analog $La_{0.7}Y_{0.3}NiSn$: difference of the volume thermal expansion coefficients (*1*) and difference of the linear thermal expansion coefficients along the *c* axis (*2*), the *b* axis (*3*), and the *a* axis (*4*).

obtained in Ref. 3 for LaNiSn agree with the data obtained in the present work. It is clear from Fig. 9 that the temperature dependences $C(T)$ of the two samples are, on the whole, similar, but the heat capacity of LaNiSn is higher than that of $La_{0.7}Y_{0.3}NiSn$ over the entire temperature range. In the temperature range 3–7 K, the temperature dependence of the heat capacity is described well by the standard law for metals: $C(T)=\gamma T+\beta T^3$ (see inset in Fig. 9). When yttrium is introduced into the lattice of LaNiSn, the electronic coefficient of the heat capacity γ decreases from 13.5 to 10 mJ/(K^2·mole), and the coefficient β of the cubic term in the heat capacity decreases by approximately 30%. This change in the values of γ and β is larger than expected on the basis of the mass of the atoms and the change in the cell volume. It should be noted that when yttrium ions replace cerium ions, which results in a smaller cell volume, the phonon spectrum determined from the heat-capacity measurements is "hardened." The "softening" of the low-energy peak in $\tilde{G}(E)$ of CeNiSn is therefore most likely due to the presence of cerium ions with unstable valence. Unfortunately, because the mass of the Y atoms is substantially different from that of the La atoms, which can strongly influence the lattice dynamics, it is undesirable to use $La_{0.7}Y_{0.3}NiSn$ as a lattice analog when measuring the phonon spectra.

It should be noted that introducing 30% La into CeNiSn does not give rise to any qualitative changes in the temperature dependence of the thermal expansion (according to a comparison of CeNiSn and $Ce_{0.7}La_{0.3}NiSn$ samples). This shows that the suppression of the gap in the electron spectrum upon introduction of La is not associated with a change in the lattice properties, at least over the temperature range 10–300 K.

To separate the contribution of delocalized $4f$-electrons of cerium to the thermal expansion of CeNiSn, a sample of $La_{0.7}Y_{0.3}NiSn$, whose cell volume is the same as that of CeNiSn and for which, importantly, $c>a$, just as for CeNiSn, was used as the nonmagnetic structural analog. The differences in the linear thermal expansion coefficients of these systems (Fig. 10) $\Delta\alpha_a$ and $\Delta\alpha_b$ have maxima at $T\approx 40$–50 K, and $\Delta\alpha_c$ has a minimum at $T\approx 20$ K. The characteristic temperatures of these features are close to the temperature of spin fluctuations (as determined from the magnetic scattering of neutrons), which indicates that they are associated with the temperature dependence of the occupancy of the $4f$ shell. The difference in the signs of the extrema for *a*, *b*, and *c* may be due to lattice anisotropy.

The difference in the volume thermal expansion coefficients of cerium and lanthanum–yttrium compounds indicates that the delocalized $4f$-electrons of cerium also contribute to the thermal expansion coefficient at temperatures above the energy of spin fluctuations. This contribution is probably determined by the influence of the delocalized $4f$-electrons of cerium on the interionic interaction potential and is not directly associated with the change in cerium valence with increasing temperature [the valence changes considerably at temperatures close to E^* (Ref. 25)]. The closeness of the volume thermal expansion coefficients of CeNiSn and LaNiSn[7,10] over the entire temperature range must be regarded as accidental: in the case of the CeNiSn system, an additional contribution to the volume thermal expansion coefficient, as compared to that of $La_{0.7}Y_{0.3}NiSn$, is determined by effects associated with the presence of partially delocalized $4f$-electrons. For LaNiSn the lattice properties give rise to the similar temperature dependence of this coefficient.

On the basis of the approach developed in Ref. 17 for Ni-bearing systems, an important parameter associated with the intermediate-valence state is the distance from the rare-earth ion to the nearest neighboring ions whose valence electrons form the conduction band. Figure 11 displays the thermal expansion coefficients for the shortest R–Ni and R–Sn distances in the RNiSn (R=Ce, La, Y) lattices, as determined from the temperature dependences of the lattice parameters using the coordination indicated in Ref. 6 for atoms in the unit cell of CeNiSn. Comparing the data on the thermal ex-

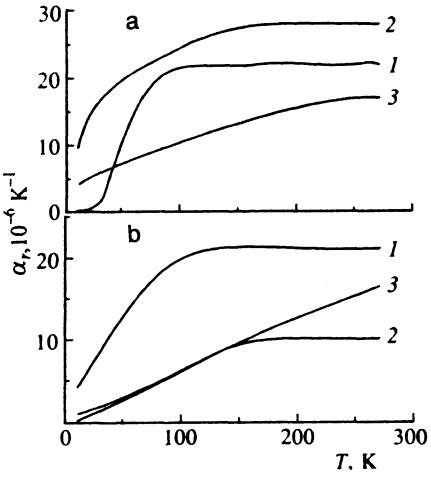

FIG. 11. Thermal expansion coefficients for the shortest distances R–Ni (a) and R–Sn (b) in the compounds CeNiSn (*1*), LaNiSn (*2*), and $La_{0.7}Y_{0.3}NiSn$ (*3*), as determined from the temperature dependence of the lattice parameters of these systems and coordinations of the atoms in the unit cell of CeNiSn.[6]

pansion coefficients for the cerium system and lanthanum-yttrium compounds suggests that, on the whole, the contribution of the $4f$ electron subsystem to the interionic interaction potential is manifested in the Ce–Sn distance (curve *1* in Fig. 11b) over a wide temperature range, right up to $T=300$ K. At temperatures of the order of E^*, the thermal expansion coefficient for the nearest distance Ce–Ni in CeNiSn is different from the thermal expansion coefficient for the nearest distance R–Ni in $La_{0.7}Y_{0.3}NiSn$ (Fig. 11a). This difference may be associated with the change in the occupancy of the $4f$-shell of the cerium ions with increasing temperature.[25]

4. CONCLUSIONS

The spectrum obtained for the magnetic excitations in the CeNiSn system by means of inelastic neutron scattering suggests that the Ce ions in this compound are in an unstable-valence state that cannot be classified as a typical state for intermediate-valence or heavy-fermion compounds. The width of the quasielastic magnetic spectral response and its temperature-dependence indicate that the CeNiSn system falls between the classical intermediate-valence and heavy-fermion systems. The characteristic energy of Kondo spin fluctuations in this compound is 4 meV.

According to L_{III} spectroscopy, the valence of Ce at $T=300$ K is 3.12 ± 0.04 and does not change when Ce is replaced by La, even at high La concentrations. The lack of such a transition may be due to the fact that the change in distance between Ce and the nearest ions when Ce is replaced by La is small.

The lack of differences between the parameters of the intermediate-valence state of Ce ions for samples in which the electron density of states contains a gap and those samples in which this gap is suppressed (at La concentrations greater than 0.1) is important evidence that the gap is produced by a coherent mechanism.

The splitting scheme (the energies and wave functions of states in the $4f$-multiplet) for C^{3+} ions in the crystal field of RNiSn was calculated. It was found that the splitting between the ground and first excited doublets (4.4 meV) is close to the Kondo energy of the CeNiSn system (about 4 meV according to the results of this work). This is important for understanding the conditions of formation of the properties of the electronic subsystem of CeNiSn. The experimental results obtained substantiate the hypothesis of Ref. 26 that a pseudogap forms by a coherent mechanism as a result of hybridization of the crystal-field excitations with Kondo excitations.

It was found that the linear thermal expansion coefficients of cerium compounds are qualitatively different from those of lanthanum compounds. This difference is due to both the peculiarity of the labile LaNiSn lattice and the valence instability of cerium.

In conclusion, we thank F. G. Aliev and R. V. Skolozdra for stimulating discussions and for providing a number of samples, O. D. Chistyakov and N. B. Kol'chugin for preparing the samples, K. A. Kikoin and E. A. Goremychkin for fruitful discussions, and I. N. Goncharenko for assisting in obtaining the neutron diffraction patterns. P. A. Alekseev thanks LRN (PSI) for support in performing the neutron experiments.

This work was performed with financial support from the International Science Fund (Grant No. M13000). E. S. Klement'ev, V. N. Lazukov, and E. V. Nefedova are grateful to the scientific management of the Russian Scientific Center for financial support.

[1] Z. Fisk, P. C. Canfield, D. J. Thompson, and M. F. Hudley, J. Alloys Compounds **181**, 369 (1992).
[2] T. Takabatake and H. Fujii, Jpn. J. Appl. Phys. **83**, 254 (1993).
[3] T. Takabatake, F. Teshima, H. Fujii *et al.*, Phys. Rev. B **41**, 9607 (1990).
[4] F. G. Aliev, R. Villard, S. Vieira *et al.*, Phys. Rev. B **47**, 769 (1993).
[5] R. V. Skolozdra, O. E. Koretskaya, and Yu. K. Gorelenko, Izv. Akad. Nauk SSSR, Neorg. Mater. **20**, 604 (1984).
[6] I. Higashi, K. Kobayashi, T. Takabatake, and M. Kasaya, J. Alloys Compounds **193**, 300 (1993).
[7] F. G. Aliev, V. V. Moshchalkov, R. V. Skolozdra (Scolozdra) *et al.*, J. Moscow Phys. Soc. **1**, 311 (1990).
[8] M. N. Khlopkin, N. A. Chernoplekov, and P. A. Cheremnykh, Preprint No. IAÉ-3549/10, Institute of Atomic Energy, Moscow (1982).
[9] N. N. Efremova, L. D. Finkel'shteĭn, N. D. Samsonova *et al.*, Izv. Akad. Nauk SSSR, Ser. Fiz. **40**, 420 (1976).
[10] P. A. Alekseev, E. S. Klement'ev (Clementyev), V. N. Lazukov, I. P. Sadikov *et al.*, Physica B **186–188**, 416 (1993).
[11] T. E. Mason, G. Aeppli, A. P. Ramirez *et al.*, Phys. Rev. Lett. **69**, 490 (1992).
[12] H. Kadowaki, T. Sato, H. Yoshizawa *et al.*, Preprint of ISSP, University of Tokyo Ser. A, 2789 (1994).
[13] J. M. Lawrence, P. S. Riseborough, and R. D. Parks, Rev. Prog. Phys. **44**, 1 (1981).
[14] E. Holland-Moritz, J. Magn. Magn. Mater. **47–48**, 127 (1985).
[15] E. Holland-Moritz, D. Wohlleben, and M. Loewenhaupt, Phys. Rev. B **25**, 7482 (1982).
[16] G. F. Aliev, N. B. Brandt, V. V. Moshchalkov *et al.*, JETP Lett. **48**, 580 (1988).
[17] P. A. Alekseev, E. S. Klement'ev, V. N. Lazukov *et al.*, Fiz. Met. Metalloved. **6**, 430 (1994).
[18] M. Kohgi, K. Ohoyama, T. Osabake *et al.*, Physica B **186–188**, 409 (1993).

[19] P. A. Alekseev, V. N. Lazukov, A. Yu. Rumyantsev, and I. P. Sadikov, J. Magn. Magn. Mater. **75**, 323 (1988).
[20] M. Blume, A. J. Freeman, and R. E. Watson, J. Chem. Phys. **37**, 1245 (1962).
[21] M. T. Hutchings, Solid State Phys. **16**, 227 (1964).
[22] U. Walter, J. Phys. Chem. Solids **45**, 401 (1984).
[23] A. Severing, W. Reichardt, E. Holland-Moritz *et al.*, Phys. Rev. B **38**, 1773 (1988).
[24] Y. Kuramoto and E. Muller-Hartman in *Valence Fluctuations in Solids*, L. M. Falikov (ed.), North-Holland, Amsterdam (1981), p. 139.
[25] N. E. Bickers, D. L. Cox, and J. W. Wilkins, Phys. Rev. B **36**, 2036 (1987).
[26] Yu. Kagan, K. A. Kikoin, and N. V. Prokof'ev, JETP Lett. **57**, 600 (1993).

Translated by M. E. Alferieff